Evidence for newly closed magnetosheath field lines at the dayside magnetopause under northward IMF

B. Lavraud,[1] M. F. Thomsen,[1] B. Lefebvre,[2] S. J. Schwartz,[2] K. Seki,[3] T. D. Phan,[4] Y. L. Wang,[1] A. Fazakerley,[5] H. Rème,[6] and A. Balogh[2]

Received 13 June 2005; revised 27 January 2006; accepted 1 February 2006; published 26 May 2006.

[1] We analyze the structure of the high-latitude magnetopause under steady interplanetary magnetic field (IMF). We use 56 magnetopause encounters of Cluster spacecraft from 2001 to 2003 to explore the statistical properties of the magnetosheath electron boundary layer, observed outside the high-latitude dayside magnetopause. We focus on the occurrence of low absolute parallel heat flux in this layer and its dependence on the magnetic field clock angle simultaneously measured by Cluster. The low absolute parallel heat fluxes result from the presence of bidirectional heated electrons in the magnetosheath electron boundary layer and are primarily observed when the local magnetic field is northward. The bidirectional heated electrons are interpreted as the signature of newly closed magnetosheath field lines that have reconnected at the high-latitude magnetopause, tailward of the cusp, in both hemispheres. This study strongly suggests that double high-latitude reconnection is a tenable mechanism for the formation of the low-latitude boundary layer and potentially of the cold, dense plasma sheet under northward IMF. Although the efficiency (in terms of mass and energy transfer) of this mechanism is still to be investigated, it is an obvious way of capturing solar wind plasma under northward IMF.

Citation: Lavraud, B., M. F. Thomsen, B. Lefebvre, S. J. Schwartz, K. Seki, T. D. Phan, Y. L. Wang, A. Fazakerley, H. Rème, and A. Balogh (2006), Evidence for newly closed magnetosheath field lines at the dayside magnetopause under northward IMF, *J. Geophys. Res.*, *111*, A05211, doi:10.1029/2005JA011266.

1. Introduction

[2] The magnetospheric boundary layer of the magnetopause has been studied extensively [e.g., *Eastman and Hones*, 1979; *Mitchell et al.*, 1987]. Its presence has been related to a number of processes, of which magnetic reconnection, diffusive entry, and Kelvin-Helmholtz instability are the leading candidates [e.g., *Eastman and Hones*, 1979; *Mitchell et al.*, 1987; *Song and Russell*, 1992; *Paschmann et al.*, 1993; *Sibeck et al.*, 1999; *Hasegawa et al.*, 2004]. In the case of magnetic reconnection, the admixture of magnetosheath and magnetospheric plasmas on magnetospheric field lines, inside the magnetopause, has been attributed to an open magnetic field topology where the magnetopause is an open boundary (e.g., rotational discontinuity) allowing plasma to flow through it. This reconnected topology also results in a boundary layer of reconnected field lines outside of the magnetopause: the magnetosheath boundary layer [*Fuselier et al.*, 1997]. The open magnetic topology leads to the presence of leaking magnetospheric particles in this layer. Furthermore, heated magnetosheath plasma is also observed in this layer and has been interpreted as having twice passed through the open magnetopause [*Fuselier et al.*, 1997].

[3] Under northward IMF, high-latitude reconnection likely occurs at the magnetopause tailward of the cusps [*Kessel et al.*, 1996]. *Song and Russell* [1992] proposed that the formation of the low-latitude boundary layer may be the result of this mechanism occurring nearly simultaneously in both hemispheres. This prediction was later given support through satellite observations [*Le et al.*, 1996; *Onsager et al.*, 2001] and MHD simulations [e.g., *Ogino et al.*, 1994; *Fedder and Lyon*, 1995; *Raeder et al.*, 1997; *Song et al.*, 1999]. On the basis of a detailed event study, *Onsager et al.* [2001] suggested that the presence of heated magnetosheath electrons streaming (unidirectional) in the magnetosheath boundary layer, outside the magnetopause at high latitudes under northward IMF, is the signature of high-latitude reconnection. They further proposed that the observation of bidirectional heated electrons there is the result of reconnection having occurred in both hemispheres.

[4] *Lavraud et al.* [2005] performed a statistical survey of the directionality of heated, streaming electrons in the magnetosheath boundary layer under steady northward IMF. Their presence and directionality was consistently shown to be the result of magnetic reconnection having occurred tailward of the cusp in one hemisphere, while not

[1]Space Science and Applications, Los Alamos National Laboratory, Los Alamos, New Mexico, USA.
[2]Blackett Laboratory, Imperial College, London, UK.
[3]Solar-Terrestrial Environment Laboratory, University of Nagoya, Aichi, Japan.
[4]Space Sciences Laboratory, University of California, Berkeley, Berkeley, California, USA.
[5]Mullard Space Science Laboratory, Surrey, UK.
[6]Centre d'Etude Spatiale des Rayonnements, Toulouse, France.

0148-0227/06/2005JA011266$09.00

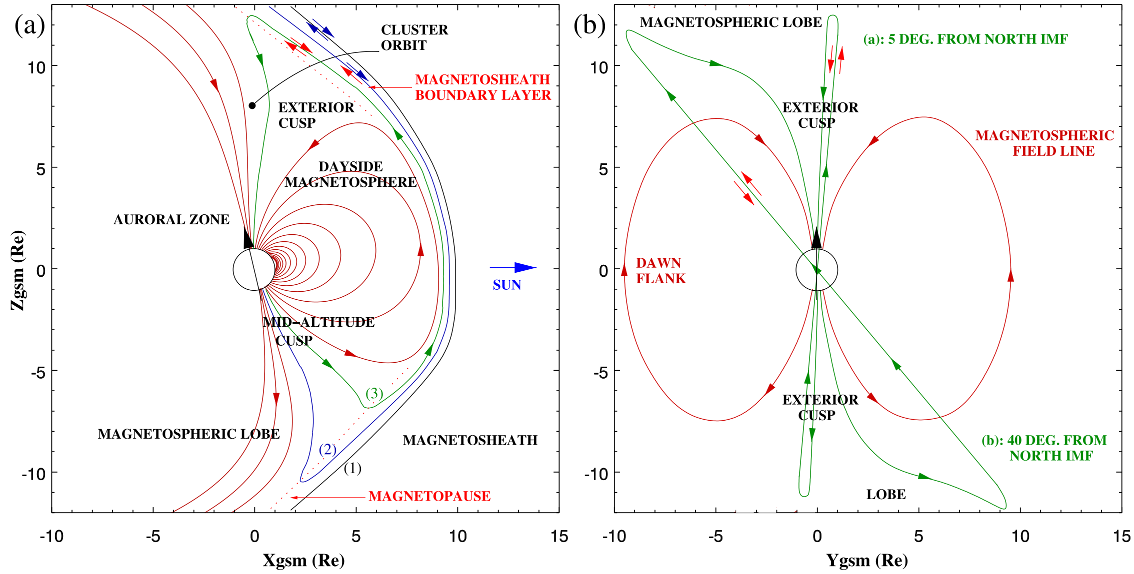

Figure 1. Schematics of the dayside magnetosphere magnetic topology under northward IMF. (a) Illustration of the high-latitude magnetopause and magnetosheath boundary layer structure under northward IMF in the context of double high-latitude reconnection. The blue arrows (top of the sketch) adjacent to the field lines numbered 1 and 2 illustrate the presence and direction of streaming, cold magnetosheath electrons. The red arrows, on field lines numbered 2 and 3, correspond to streaming heated electrons. Field line 1 is a pristine magnetosheath field line. Field line 2 is a magnetosheath field line which has reconnected in one hemisphere (southern in the present example). Field line 3 has reconnected in the lobes of both hemispheres and is thus newly closed. (b) Illustration of the effect of a nonpurely northward IMF on the occurrence of double high-latitude reconnection. For a small magnetosheath magnetic field clock angle of 5° (field line labeled "a"), reconnection in both hemispheres may easily occur. For larger clock angles, such as −40° for field line labeled "b," this process may also occur. However, the larger the clock angle, the smaller the chance of reconnecting in both hemispheres and this probability ought to vanish when approaching 90°.

yet in the other. Furthermore, the hemisphere of initial reconnection was shown to be primarily controlled by the dipole tilt angle. *Lavraud et al.* [2005] also highlighted the possible signature of magnetosheath field lines having reconnected in both hemispheres and listed potential candidates. Identification was based on electron temperatures being elevated in both parallel and anti-parallel direction (i.e., low heat flux) in the presence of undisturbed magnetosheath ion populations (low temperature). By contrast, the layers of unidirectional heated electrons they analyzed were suggestive of higher parallel heat fluxes.

[5] Figure 1a illustrates the magnetic structure (topology) of the magnetopause if reconnection of a given magnetosheath field line (labeled 1) occurs in both hemispheres under purely northward IMF. In the case shown here, magnetosheath field lines may reconnect first in the southern hemisphere (field line 2) (see also *Lavraud et al.* [2005]). The same field line may later reconnect in the opposite hemisphere and create a newly closed field line (field line 3). This mechanism may hold not only for purely northward IMF, but also for a range of IMF clock angles extending each side of the purely northward direction. Figure 1b illustrates such a possible influence of the IMF clock angle ($\tan^{-1}(B_Y/B_Z)$). The (quasi) purely northward IMF (clock angle of 5°) case is represented by field line a. The field line labeled b has a magnetosheath clock angle of −40°. This field line is antiparallel to the magnetospheric field near the cusps in both hemispheres and would potentially reconnect in the dawn (dusk) quadrant for the northern (southern) hemisphere.

[6] In this paper, we study the combined occurrence of low absolute parallel electron heat flux and parallel heated electrons in the magnetosheath boundary layer, as a function of the local magnetic field clock angle, to assess the tenability of the mechanism proposed by *Song and Russell* [1992]. We will show direct statistical evidence (in situ observations) of the occurrence of this mechanism, which has been suggested as a way to form the low-latitude boundary layer as well as the cold, dense plasma sheet [e.g., *Lavraud et al.*, 2005; *Li et al.*, 2005; *Øieroset et al.*, 2005].

2. Instrumentation and Definitions

2.1. Instrumentation

[7] We primarily use electron data from the PEACE (Plasma Electron and Current Experiment) instrument on board Cluster [*Johnstone et al.*, 1997]. The data come from the LEEA (Low Energy Electron Analyzer) sensor which measures electrons in the energy range 0.6 eV to 1 keV. We use electron temperature and parallel heat flux moments which were computed from onboard-selected two-dimensional (2-D) pitch angle data. Photoelectrons were removed by use of a lower energy cutoff equal to the

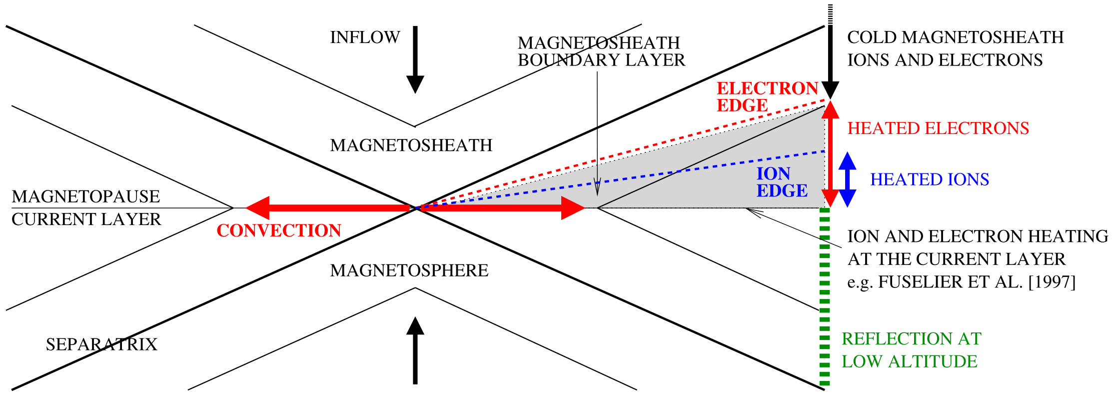

Figure 2. Illustration of the structure of the reconnected magnetopause. The magnetopause current layer is represented as a thin horizontal black line (labeled on the left-hand side of the plot). The magnetosheath is located in the upper portion of the schematic while the magnetosphere is the lower portion. Magnetic field lines are drawn as thin black lines with the separatrix (passing through the reconnection site) being thicker. Reconnection induces a convection directed away from the reconnection region each side of the reconnection line as indicated by the red arrows. Ions and electrons are heated at the magnetopause current layer. This does not necessarily happen only near the reconnection region but rather all along the magnetopause current layer [e.g., *Fuselier et al.*, 1997; *Onsager et al.*, 2001]. The magnetosheath boundary layer results from a velocity filter effect which produces an electron edge further on the magnetosheath side than the ion edge [*Gosling et al.*, 1990]. The magnetosheath boundary layer thus contains heated particles which delineate separate ion and electron edges as a combined result of (a) particle passage through the magnetopause, reflection at low altitude and subsequent escape back through the magnetopause, (b) direct escape of hot magnetospheric particles originally trapped on dayside closed field lines [*Gosling et al.*, 1990] and (c) direct reflection at the magnetopause current layer [*Fuselier et al.*, 1991] (see text for details). The eventuality of double high-latitude reconnection is described in the text.

floating spacecraft potential when available (7 eV otherwise). Cluster Ion Spectrometry/Hot Ion Analyser (CIS/HIA) [*Rème et al.*, 2001] and Flux Gate Magnetometer (FGM) [*Balogh et al.*, 2001] data were also utilized for the analyses. This study makes use of perpendicular ion temperature only. The use of the parallel ion temperature leads to similar results. Only data from Cluster spacecraft 3 are used in the present study. Data resolution is 4 s, except during 2001 when it is 20 s (see section 3.2).

2.2. Magnetosheath Boundary Layer and Magnetopause

[8] Figure 2 illustrates schematically the open magnetopause structure that forms the interpretive foundation for our investigation. Observations show that magnetosheath plasma is heated upon traversal of the magnetopause current layer [*Paschmann et al.*, 1993; *Phan et al.*, 1994; *Fuselier et al.*, 1997]. Potential plasma heating mechanisms have been studied by *Lee et al.* [1994] and *Johnson and Cheng* [1997, 2001]. Both heated magnetosheath ions and electrons may enter the magnetosphere at the onset of reconnection (and thereafter along the open magnetopause), mirror at low altitude, and return to the magnetopause. From there, they may escape back into the magnetosheath, through the open magnetopause, to form an observable magnetosheath boundary layer outside of the main current layer. The convection imposed by reconnection, combined with the finite field-aligned velocity of the entering/escaping particles, results in a velocity filter effect. Because electrons are much faster than ions, this effect leads to a layered structure where heated magnetosheath electrons form the outermost layer of the open magnetopause. This layer is characterized by heated magnetosheath electrons streaming away from the magnetopause (grey area in Figure 2) [*Fuselier et al.*, 1997]. Heated magnetosheath ions are not yet present in this layer due to their lower velocities. These also form a similar layer, but its outer edge is closer to the magnetopause current layer [*Gosling et al.*, 1990]. In addition to the scenario described above, the magnetosheath boundary layer structure may also result from (1) the direct escape of hot magnetospheric particles originally trapped on dayside closed field lines (primarily for the southward IMF case) [*Gosling et al.*, 1990] and (2) the direct reflection of particles at the magnetopause current layer [*Fuselier et al.*, 1991]. All these effects produce distinct ion and electron edges located outside the magnetopause current layer (see Figure 2), and correspond to temperature enhancements observable in the respective distribution functions (see section 3.2 for an event illustration).

[9] As shown in Figure 2, the magnetopause is identified as the current layer where the main magnetic field rotation occurs. However, in many of the crossings we study here (particularly those under northward IMF) there is little discernable magnetic shear. Therefore we use the increase in the ion temperature as a proxy for the actual magnetopause, realizing that in the open geometry this transition lies somewhat outside the magnetopause. With this working definition, we then identify the magnetosheath electron boundary layer by elevated electron temperatures while the ion temperature retains its magnetosheath value.

[10] The schematic of Figure 2 illustrates the magnetosheath boundary layer for either a reconnection site located at high latitude under northward IMF or low latitude under southward IMF. However, it does not describe the case of possible double high-latitude reconnection. As discussed by *Onsager et al.* [2001], under northward IMF and in the presence of newly closed field lines, the expected electron signatures of the different regions from the magnetosheath inward are as follows (cf. Figure 1a and Figure 2): (1) pristine magnetosheath field lines disconnected from Earth, with typical cold magnetosheath electrons in all directions, (2) magnetosheath boundary layer field lines with one end connected to the Earth, and characterized by heated streaming electrons in one direction (parallel or antiparallel) and cold magnetosheath electrons in the other, (3) newly closed magnetosheath boundary layer field lines with both ends connected to Earth and with heated electrons in both directions along the field lines, i.e., with balanced fluxes, and (4) low-latitude boundary layer (or cusp) field lines with similar balanced heated electron fluxes but located inside the magnetopause. Such electron properties can be associated with characteristic signatures in the appropriate moments of the electron distribution functions in the following manner, and in the same order: (1) typical, low magnetosheath electron and ion temperatures with arbitrary electron heat flux, (2) low ion temperature, but higher electron temperature with high (parallel or antiparallel) heat flux due to the streaming, (3) low ion temperature with high electron temperature and low heat flux owing to balanced electron fluxes, and (4) high electron temperature and low heat flux, but high ion temperatures as well starting once the spacecraft encounters the ion edge of the magnetosheath boundary layer. With this association (illustrated in section 3.2), we base our study on the quantitative analysis of the appropriate moments of the ion and electron distributions.

3. Event Selection and Statistical Analysis

3.1. Event Selection

[11] We used magnetic field and ion observations to identify all spacecraft 3 magnetopause crossings from the first three years of Cluster operation (2001–2003), between January and May (dayside). We used time-lagged ACE solar wind measurements (cf. *Lavraud et al.* [2005] for details) and selected the events for which the IMF clock angle ($\tan^{-1}(B_Y/B_Z)$ in GSM) was steady, varying by less than 30° during a 30-min interval centered on each magnetopause crossing. This selection criterion avoids variable events for which dynamic effects may prevent the formation of a steady boundary layer. Fifty-six events met these criteria and had good data from all instruments.

3.2. Event Illustration

[12] Figure 3 presents Cluster spacecraft 3 observations from PEACE, CIS and FGM for the high-latitude southern hemisphere magnetopause crossing on 4 May 2002. The details may be found in the figure caption. This event is one of the 56 events selected.

[13] At the start of the interval, Cluster spacecraft 3 was in the magnetosheath and observed low ion and electron temperatures and large plasma flows (Figures 3e, 3f, and 3h). This is an inbound pass in the southern hemisphere. The entry into the magnetosheath electron boundary layer occurred at ~1403 UT. This is indicated by the increase in the spectral width of electron distributions in Figures 3a, 3b, and 3c, and the corresponding increase in the parallel electron temperatures in Figure 3h. Within the magnetosheath electron boundary layer (until ~1415 UT), the ion temperature is generally low and typical of the magnetosheath. Electrons in this boundary layer are mostly seen to be heated in both parallel and antiparallel directions, with generally low parallel heat flux (Figure 3g), so that by the above interpretation, most of the interval until ~1416 UT (see next paragraph for magnetopause current layer signatures) presumably corresponds to a newly closed magnetosheath boundary layer (region 3 from section 2.2 and Figure 1a). At times, however, more unidirectional heated electrons are observed, e.g., 1408–1409 UT (see also examples by *Onsager et al.* [2001] and *Lavraud et al.* [2005]). These presumably correspond to field lines that are reconnected in only one hemisphere.

[14] The magnetopause current layer crossing is observed at ~1416 UT (second dotted vertical line in Figure 3) as a slight rotation in the magnetic field components (B_X in particular) together with a net decrease in the ion flow speed (Figures 3e and 3i). The ion perpendicular temperature is low in the magnetosheath but increases abruptly on approach to the magnetopause (first dotted vertical line in Figure 3). The red arrows indicate the times for which four selected ion distribution functions are shown in Figure 4. Figure 4a displays a typical, cold, streaming magnetosheath ion distribution. Figure 4b is a similar cold magnetosheath distribution but corresponds to a time when electrons are already substantially heated: the magnetosheath electron-only boundary layer (c.f. Figure 2). Figure 4c displays an ion distribution close to the increase in ion temperature at 1414:52 UT. This distribution shows the appearance of counterstreaming ions. These may be interpreted as heated and/or reflected magnetosheath ions returning to the spacecraft from the open magnetopause [*Fuselier et al.*, 1991]. Finally, Figure 4d shows that ions inside the magnetopause are both hot and isotropic, as also found by *Lavraud et al.* [2002]. These observations are all compatible with expectations from the boundary layer structure described in section 2, in which the ion edge of the magnetosheath boundary layer should be much closer to the magnetopause than the electron edge.

[15] The observation of heated magnetosheath electrons together with colder ions thus appears as an unambiguous signature that the spacecraft is outside the magnetopause. In Figures 3f, 3g, and 3h, the dashed green lines correspond to the threshold used for the analysis described in section 3.3. Times where the analysis identifies doubly-reconnected field lines during the event of 4 May 2002 are displayed as asterisks at the bottom of Figure 3g.

3.3. Events Analysis

[16] For each of the 56 events, we selected a time interval starting from the boundary layer (or cusp) well inside the magnetopause and ending in typical magnetosheath. The times were selected so that the perpendicular ion temperatures in the inner boundary layer and magnetosheath were typical of each region (generally about several hundred eV

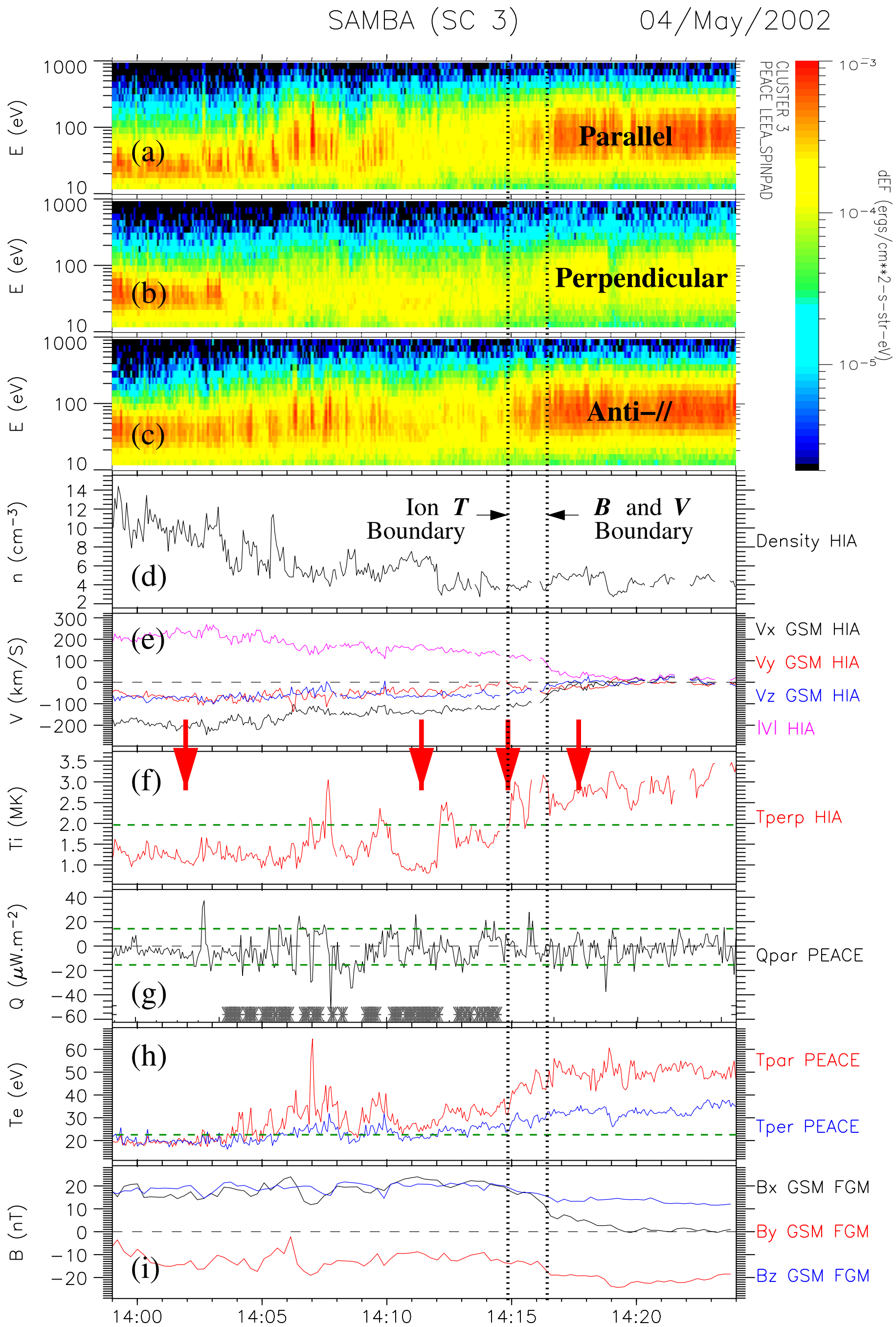

Figure 3. Overview plot of PEACE, CIS and FGM data for the southern hemisphere magnetopause crossing interval on 4 May 2002. The location of the spacecraft at 1410 UT is (1.3, −8.0, −10.4) R_E in GSM or (5.4, −8.0, −9.0) R_E in SM coordinates. (a), (b), and (c) Three spectrograms are shown for electrons flowing parallel, perpendicular, and antiparallel to the magnetic field, respectively. (d), (e) and (f) The CIS/HIA ion density, velocity components (in GSM) and magnitude, and perpendicular temperature, respectively. (f) The dashed green line represents the ion temperature threshold used to define magnetosheath measurements. (g) The parallel electron heat flux and (h) the parallel and perpendicular electron temperatures. In Figure 3g, the dashed green lines delimit the thresholds of −15 and +15 $\mu W/m^2$ used in the statistical analysis. In Figure 3h, the threshold of 1.1 for parallel electron temperature enhancement is shown. (i) FGM magnetic field measurements (GSM). The asterisks at the bottom of Figure 3g show the times at which electron heat flux, anisotropy and temperature ratio criteria (c.f. section 3.4) are met in the magnetosheath (i.e., for ion temperatures lower than threshold). Two vertical dotted lines indicate the location of the current layer (observable in both magnetic field and velocity) and of the ion temperature boundary. The four red arrows mark the times of the ion distribution functions of Figure 4. See text for further details.

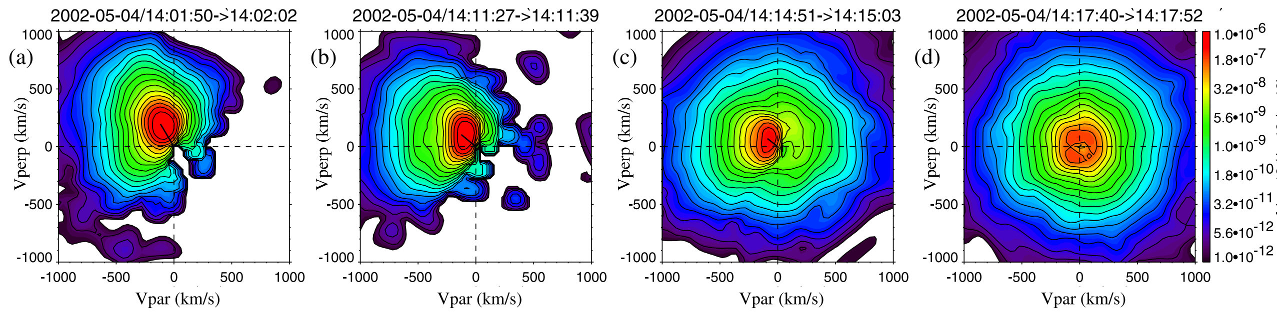

Figure 4. Ion distribution functions from the CIS/HIA instruments for four selected times during the magnetopause crossing on 4 May 2002. These are two-dimensional cuts of the distributions in the ($V_{\|}$, $V_{\perp}$) plane. The times are given in each plot and are marked by red arrows on Figure 3.

and a hundred eV, respectively). Averaged over 20 s from the beginning and the end of each interval, these two temperatures were used as reference. The spacecraft location is deemed to be outside the magnetopause (i.e., "magnetosheath") if the perpendicular ion temperature is less than a threshold value, taken to be the magnetosheath ion temperature of reference plus a quarter of the difference between the inner boundary layer and magnetosheath ion temperatures of reference (i.e., $T < T_{SH} + (T_{BL} - T_{SH})/4$; see Figure 3f for illustration). Then the parallel electron heat fluxes and electron temperatures from PEACE and the magnetic field clock angles from both FGM and ACE were interpolated to the times of the ion measurements. We made the interpolation onto the ion measurement time tags because this dataset contains a number of data gaps. Electron data from 2001 have a resolution of 20 s owing to onboard calculation issues (12 events out of 56). In this case, the interpolation was made to the electron measurement time tags, resulting in fewer measurements to analyze. Thus, the statistical weight of the events from 2001 is a factor of 4 lower than those of 2002 and 2003.

[17] Figure 5a shows a scatter plot of the parallel electron heat flux as a function of the parallel electron temperature normalized to the reference parallel electron temperature of the magnetosheath. Only measurements defined as magnetosheath, based on the ion temperature criteria, are displayed. A normalized temperature significantly higher than one indicates the presence of heated electrons in the magnetosheath. Figure 5a shows a large spread in both parallel heat flux and normalized parallel temperature. For large normalized temperature the absolute parallel heat flux is generally low. The median absolute parallel heat flux is 20.5 $\mu W/m^2$ (mean of 31.0 $\mu W/m^2$) and the median normalized temperature is 1.04 (mean of 1.09). To focus on events that may indicate double high-latitude reconnection (i.e., those with high parallel electron temperature and low parallel heat flux, outside of the magnetopause), we identify those magnetosheath measurements with a parallel heat flux $|Q_{\|}| < 15$ $\mu W/m^2$ and a normalized temperature greater

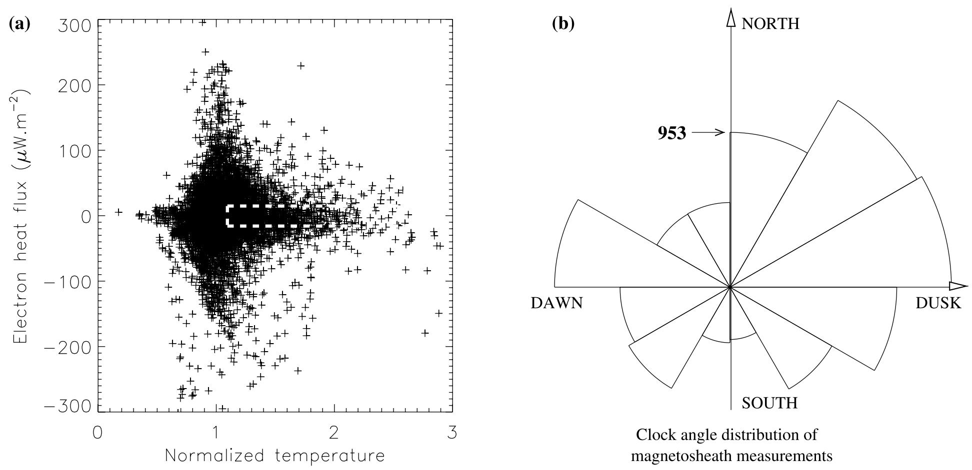

Figure 5. (a) Scatter plot of the parallel electron heat flux as a function of the ratio of the parallel electron temperature to the parallel electron temperature of the reference magnetosheath. Only measurements defined as magnetosheath are displayed (based on ion temperature). The dashed white lines delimit the threshold used in the analysis, which are respectively of $|Q_{\|}| < 15$ $\mu W/m^2$ and $T_{\|}/T_{\|SH} > 1.1$. (b) Polar distribution of the absolute occurrence of FGM clock angles for all the measurements defined as magnetosheath in our analysis. It is binned into 12 clock angle ranges of 30° each with the north direction upward and dusk toward the right-hand side. The scale is homogeneous and an absolute value is given for one of the northward bins. See text for further details.

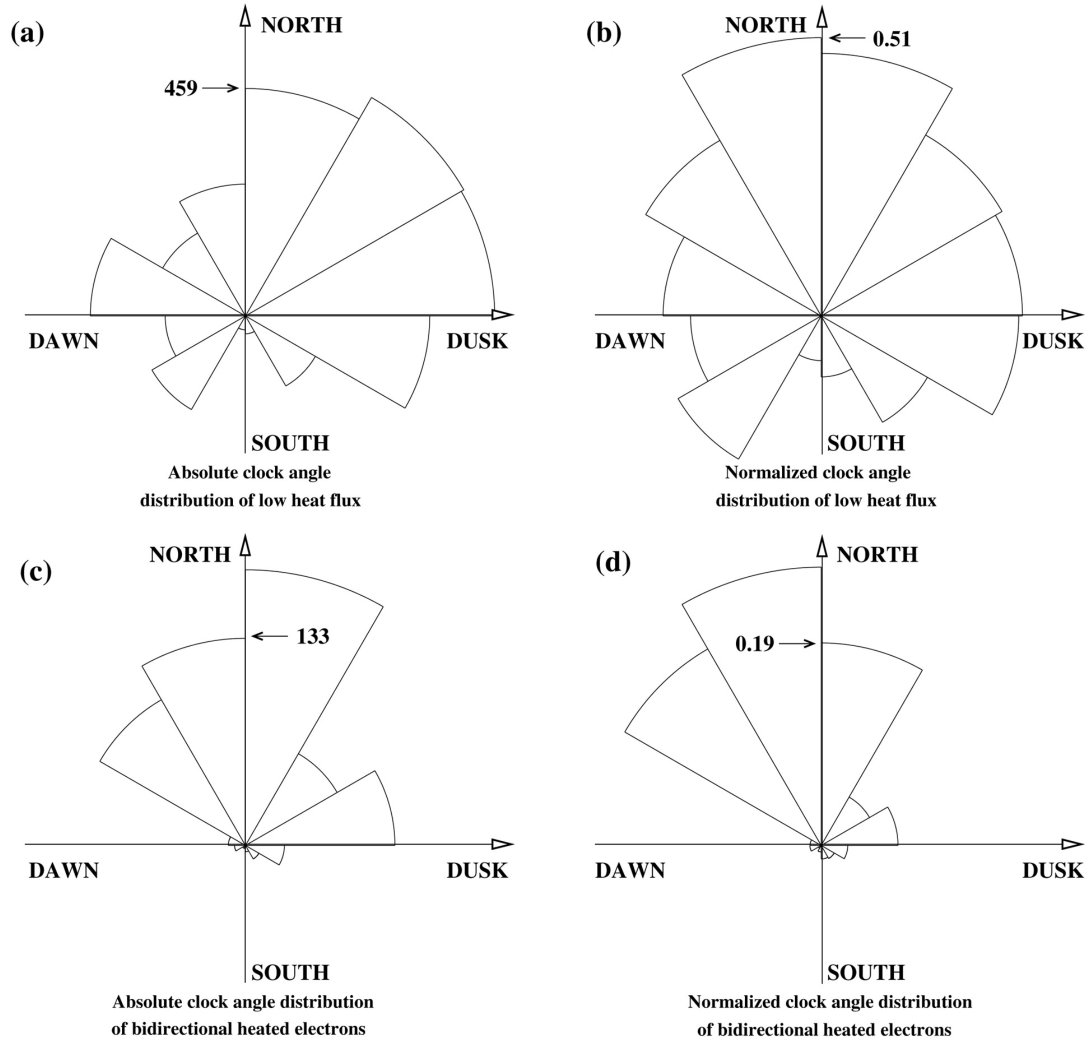

Figure 6. Results of the statistical analysis performed on the 56 magnetopause crossing events. All four plots are polar distributions of FGM magnetic field clock angle measurements, in the same format as Figure 5b. (a) Absolute clock angle distribution of all magnetosheath measurements having low parallel electron heat flux ($|Q_{||}| < 15\ \mu W/m^2$). (c) Absolute clock angle distribution of all magnetosheath measurements which meet the criteria on electron heat flux, anisotropy ($T_{||} > T_{\perp}$) and parallel electron temperature ratio (> 1.1). The distributions ((b) and (d)) are the same as Figures 6b and 6c, respectively but normalized to the original clock angle distribution of magnetosheath measurements from Figure 5b. One axis value is specified for each distribution.

than 1.1 (these criteria are shown in Figure 5a with dashed white lines). In the analysis of section 3.5, we further require an electron anisotropy such that $T_{||} > T_{\perp}$. As was illustrated in section 3.2, magnetopause electron heating results in such an anisotropy in the magnetosheath boundary layer. This latter criterion also allows us to avoid the effect of electron temperature variability in the magnetosheath. The main results of this paper do not change significantly by applying other, stricter criteria; these basically only reduce the statistics (see next section and Figure 7).

3.4. Statistical Criteria and Results

[18] The asterisks at the bottom of Figure 3g show the times at which all the selection criteria are satisfied for the magnetopause crossing on 4 May 2002. These criteria are shown as dashed green lines in Figures 3f, 3g, and 3h, and in summary correspond to (1) ion perpendicular temperature $T_{\perp} < T_{\perp SH} + (T_{\perp BL} - T_{\perp SH})/4$, (2) absolute parallel electron heat flux $|Q_{||}| < 15\ \mu W/m^2$, (3) normalized parallel electron temperature $T_{||}/T_{||SH} > 1.1$, (4) electron temperature anisotropy $T_{||} > T_{\perp}$.

[19] In addition, we require that the magnetic field measured by FGM does not vary by more than 20° between two adjacent measurements and that the above criteria be met for at least two contiguous measurements. The former is meant to avoid time aliasing, while the latter is meant to remove bad measurements. However, the main results hold even if these two requirements are not used. These criteria should be met when the spacecraft samples a closed magnetosheath electron boundary, where electrons are heated and the heat flux is low, as seen for example in Figure 3.

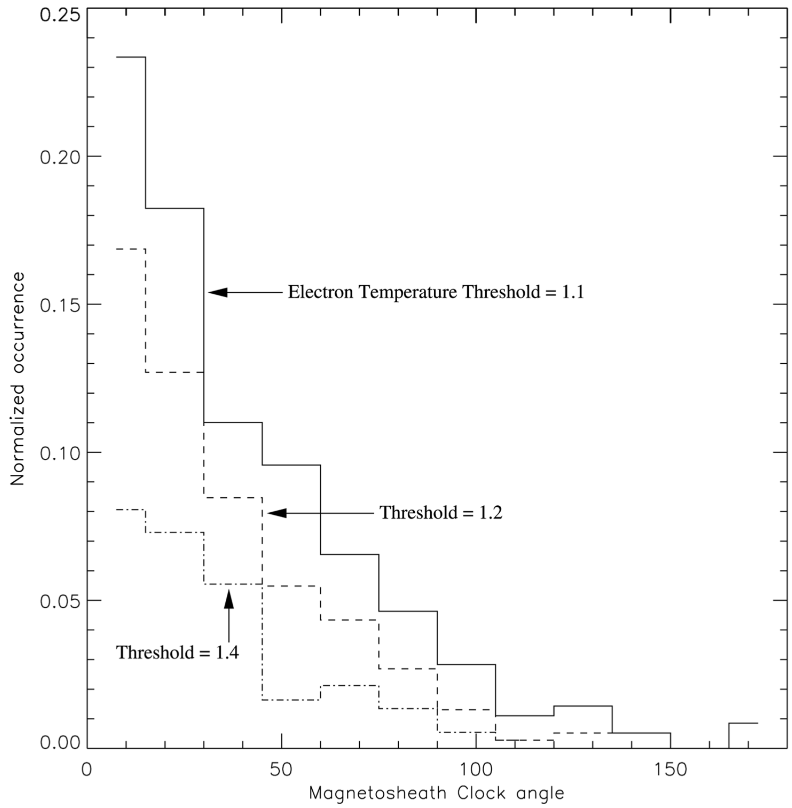

Figure 7. Histogram representation of the FGM absolute magnetosheath clock angle distributions of low heat flux heated electrons in the magnetosheath electron boundary layer. Those correspond to the result of the analysis by using an electron heating factor of 1.1 (solid), 1.2 (dashed), and 1.4 (dash-dotted), displayed in 15° bins. See text for further details.

[20] Figure 5b shows the clock angle distribution of all magnetosheath measurements, defined using the ion temperature threshold, for the 56 events of this study. This distribution shows some preference for duskward magnetic field orientation but is overall fairly evenly distributed. The polar distribution of Figure 6a shows the absolute clock angle distribution of the magnetosheath measurements that have a low absolute parallel electron heat flux. This distribution shows some tendency for low heat flux to occur under northward IMF orientation. However, the occurrence for southward IMF is not negligible. The distribution of Figure 6b is the same but normalized to the distribution of all magnetosheath measurements from Figure 5b. It shows that low electron heat flux observations in the magnetosheath are relatively evenly distributed in terms of clock angle, although some clear deficit is observed for strongly southward directions.

[21] The application of all criteria defined above results in the absolute polar distribution of Figure 6c and the normalized distribution of Figure 6d. The clock angle distribution of magnetosheath measurements satisfying the criteria is clearly confined to northward IMF. These distributions demonstrate conclusively that the combination of low parallel electron heat flux and parallel heated electrons with $T_{\parallel} > T_{\perp}$ (i.e., bidirectional heated electrons) only occurs when the magnetosheath magnetic field has a northward component. The occurrence of such measurements is strikingly low for absolute clock angles larger than 60°.

[22] As mentioned above, all magnetosheath measurements were also assigned IMF values as described in section 3.2. We checked for the compatibility between the lagged IMF monitored by ACE and the local magnetic field recorded by FGM at Cluster. The median absolute clock angle deviation between the two datasets is 15.7° (mean of 22.9°). This modest difference may be attributed to IMF passage through the bow shock and subsequent draping along the magnetopause. It thus appears that the fact that bidirectional heated electrons are almost exclusively observed for northward local magnetic field in the magnetosheath boundary layer can be more generally extended to northward IMF orientation.

[23] In the above, we presented results from the analysis using an electron temperature heating criterion of 1.1 (compared to typical sheath value). This choice primarily aimed at obtaining significant statistics. Similar analysis has been performed for different heating factors. In Figure 7 we show the absolute (i.e., in the range [0°, 180°]) magnetosheath clock angle distributions of low heat flux, heated electrons in the magnetosheath boundary layer for electron heating criteria of 1.1 (original), 1.2, and 1.4, respectively, with the solid, dashed, and dash-dotted lines. These distributions are displayed with 15° bins. It is observed that the distributions are overall smoother in this representation compared to the coarser polar plots of Figure 6. It is clear from those distributions that such observation globally becomes much less frequent for absolute clock angle greater

than 60°. It may be noted, finally, that the orbit of Cluster crosses the dayside magnetopause at rather high magnetic latitudes (∼50°–70°). This may result in the impossibility to observe newly closed boundary layers for large magnetosheath clock angles. This potential effect ought to be further examined in the future.

4. Discussion and Conclusion

[24] We have studied Cluster high-latitude magnetopause crossings under steady IMF conditions from 2001 to 2003. We have analyzed the statistical properties of the magnetosheath and searched for the presence of heated, bidirectional electrons outside the magnetopause. As a signature of such distributions, we sought a low absolute parallel electron heat flux in the presence of an elevated parallel electron temperature. We focused on the dependence of such measurements on the local magnetosheath clock angle. We illustrated our analysis with an event that occurred under northward IMF. It showed the presence of such heated, bidirectional electrons outside the magnetopause. This event also illustrated that the ion temperature is a useful parameter to identify locations outside the magnetopause. Statistical results, based on 56 magnetopause crossings, showed that low absolute parallel electron heat flux may be observed for all IMF orientations. However, the observation of combined low electron heat flux and parallel heated electrons is restricted to local magnetosheath clock angles having a northward component. The occurrence of such measurements is strikingly low for absolute clock angles greater than 60°.

[25] Visual inspection of all events confirms the finding from the event illustration. The combined occurrence of low absolute parallel heat fluxes and increased parallel electron temperature results from the presence of bidirectional heated electrons in the magnetosheath electron boundary layer. These are interpreted as the signature of high-latitude reconnection having occurred in the lobes of both hemispheres. *Twitty et al.* [2004] recently found a high-latitude reconnection occurrence rate of 90% when the IMF has a northward component (i.e., for IMF clock angles between −90° and 90°) and suggested that double high-latitude reconnection may be common. Probably owing to simple geometrical considerations, our study shows that this mechanism is mainly restricted to clock angles in the range ∼[−60°, 60°].

[26] In essence, these results strongly support the fact that bidirectional heated electrons are the signature of newly closed magnetosheath field lines and that this mechanism [*Song and Russell*, 1992] only occurs for magnetosheath magnetic field, and correlated IMF, having a significant northward component. This mechanism leads to the formation of the dayside low-latitude boundary layer and possibly of the cold, dense plasma sheet under northward IMF. However, although this mechanism is shown to be commonly operative, further work is needed to assess its efficiency in terms of mass and energy transfer, as compared to alternate processes such as the Kelvin-Helmholtz instability [*Hasegawa et al.*, 2004].

[27] **Acknowledgments.** B. L. is grateful to S. A. Fuselier, M. Maksimovic and D. Fontaine for fruitful discussions. The authors thank the ACE MFI and SWEPAM instruments teams and the CDAWeb for providing the ACE data. Work at Los Alamos was conducted under the auspices of the U.S. Department of Energy, with support from NASA programs (PEACE data analysis; Exploration of solar wind plasma entry).

[28] Lou-Chuang Lee thanks the reviewers for their assistance in evaluating this paper.

References

Balogh, A., et al. (2001), The Cluster magnetic field investigation: Overview of in-flight performance and initial results, *Ann. Geophys.*, *19*(10–12), 1207–1217.

Eastman, T. E., and E. W. Hones Jr. (1979), Characteristics of the magnetospheric boundary layer and magnetopause layer as observed by IMP 6, *J. Geophys. Res.*, *84*(A5), 2019–2028.

Fedder, J. A., and J. G. Lyon (1995), The Earth's magnetosphere is 165 R_E long: Self-consistent currents, convection, magnetospheric structure, and processes for northward interplanetary magnetic field, *J. Geophys. Res.*, *100*(A3), 3623–3635.

Fuselier, S. A., D. M. Klumpar, and E. G. Shelley (1991), Ion reflection and transmission during reconnection at the Earth's subsolar magnetopause, *Geophys. Res. Lett.*, *18*, 139–143.

Fuselier, S. A., B. J. Anderson, and T. G. Onsager (1997), Electron and ion signatures of field line topology at the low-shear magnetopause, *J. Geophys. Res.*, *102*(A3), 4847–4863.

Gosling, J. T., M. F. Thomsen, S. J. Bame, T. G. Onsager, and C. T. Russell (1990), The electron edge of the low-latitude boundary layer during accelerated flow events, *Geophys. Res. Lett.*, *17*, 1833–1836.

Hasegawa, H., et al. (2004), Rolled-up Kelvin-Helmholtz vortices and associated solar wind entry at Earth's magnetopause, *Nature*, *430*, 755–758.

Johnson, J. R., and C. Z. Cheng (1997), Kinetic Alfvén waves and plasma transport at the magnetopause, *Geophys. Res. Lett.*, *24*(11), 1423–1426.

Johnson, J. R., and C. Z. Cheng (2001), Stochastic ion heating at the magnetopause due to kinetic Alfvén waves, *Geophys. Res. Lett.*, *28*(23), 4421–4424.

Johnstone, A. D., et al. (1997), PEACE: A plasma electron and current experiment, *Space Sci. Rev.*, *79*(1–2), 351–398.

Kessel, R. L., et al. (1996), Evidence of high-latitude reconnection during northward IMF: Hawkeye observations, *Geophys. Res. Lett.*, *23*(5), 583–586.

Lavraud, B., et al. (2002), Cluster observations of the exterior cusp and its surrounding boundaries under northward IMF, *Geophys. Res. Lett.*, *29*(20), 1995, doi:10.1029/2002GL015464.

Lavraud, B., et al. (2005), Characteristics of the magnetosheath electron boundary layer under northward IMF: Implications for high-latitude reconnection, *J. Geophys. Res.*, *110*, A06209, doi:10.1029/2004JA010808.

Le, G., C. T. Russell, J. T. Gosling, and M. F. Thomsen (1996), ISEE observations of low-latitude boundary layer for northward interplanetary magnetic field: Implications for cusp reconnection, *J. Geophys. Res.*, *101*(A12), 27,239–27,249.

Lee, L. C., J. R. Johnson, and Z. W. Ma (1994), Kinetic Alfvén waves as a source of plasma transport at the dayside magnetopause, *J. Geophys. Res.*, *99*(A9), 17,405–17,411.

Li, W. H., et al. (2005), Plasma sheet formation during long period of northward IMF, *Geophys. Res. Lett.*, *32*, L12S08, doi:10.1029/2004GL021524.

Mitchell, D., et al. (1987), An extended study of the low-latitude boundary layer on the dawn and dusk flank of the magnetosphere, *J. Geophys. Res.*, *92*(A7), 7394–7404.

Ogino, T., R. J. Walker, and M. Ashourabdalla (1994), A global magnetohydrodynamic simulation of the response of the magnetosphere to a northward turning of the interplanetary magnetic field, *J. Geophys. Res.*, *99*(A6), 11,027–11,042.

Øieroset, M., et al. (2005), Global cooling and densification of the plasma sheet during an extended period of purely northward IMF on October 22–24, 2003, *Geophys. Res. Lett.*, *32*, L12S07, doi:10.1029/2004GL021523.

Onsager, T. G., J. D. Scudder, M. Lockwood, and C. T. Russell (2001), Reconnection at the high latitude magnetopause during northward interplanetary magnetic field conditions, *J. Geophys. Res.*, *106*(A11), 25,467–25,488.

Paschmann, G., W. Baumjohann, N. Sckopke, T. D. Phan, and H. Luehr (1993), Structure of the dayside magnetopause for low magnetic shear, *J. Geophys. Res.*, *98*(A8), 13,409–13,422.

Phan, T. D., G. Paschmann, W. Baumjohann, N. Sckopke, and H. Luhr (1994), The magnetosheath region adjacent to the dayside magnetopause: AMPTE/IRM observations, *J. Geophys. Res.*, *99*(A1), 121–141.

Phan, T. D., et al. (2003), Simultaneous Cluster and IMAGE observations of cusp reconnection and auroral proton spot for northward IMF, *Geophys. Res. Lett.*, *30*(10), 1509, doi:10.1029/2003GL016885.

Raeder, J., et al. (1997), Boundary layer formation in the magnetotail: Geotail observations and comparisons with a global MHD simulation, *Geophys. Res. Lett.*, *24*(8), 951–954.

Rème, H., et al. (2001), First multispacecraft ion measurements in and near the Earth's magnetosphere with the identical CLUSTER Ion Spectrometry (CIS) Experiment, *Ann. Geophys.*, *19*(10–12), 1303–1354.

Sibeck, D. G., et al. (1999), Chapter 5-plasma transfer processes at the magnetopause, *Space Sci. Rev.*, *88*, 207.

Song, P., and C. T. Russell (1992), Model of the formation of the low-latitude boundary layer for strongly northward interplanetary magnetic field, *J. Geophys. Res.*, *97*(A2), 1411–1420.

Song, P., D. L. DeZeeuw, T. I. Gombosi, C. P. T. Groth, and K. G. Powell (1999), A numerical study of the solar wind-magnetosphere interaction for northward interplanetary magnetic field, *J. Geophys. Res.*, *104*(A12), 28,361–28,378.

Twitty, C. K., et al. (2004), Cluster survey of cusp reconnection and its IMF dependence, *Geophys. Res. Lett.*, *31*, L19808, doi:10.1029/2004GL020646.

A. Balogh, B. Lefebvre, and S. J. Schwartz, Blackett Laboratory, Imperial College, London SW7 2BW, UK.

A. Fazakerley, Mullard Space Science Laboratory, Dorking, Surrey RH5 6NT, UK.

B. Lavraud, M. F. Thomsen, and Y. L. Wang, Space Science and Applications, Los Alamos National Laboratory, P.O. Box 1663, MS D466, Los Alamos, NM 87545, USA. (lavraud@lanl.gov)

T. D. Phan, Space Sciences Laboratory, University of California, Berkeley, Berkeley, CA 94720, USA.

H. Rème, Centre d'Etude Spatiale des Rayonnements, F-31028 Toulouse cedex 4, France.

K. Seki, Solar-Terrestrial Environment Laboratory, University of Nagoya, 442-8507 Aichi, Japan.